Available online at www.sciencedirect.com
ScienceDirect
Journal of Sound and Vibration 301 (2007) 236–252
JOURNAL OF SOUND AND VIBRATION
www.elsevier.com/locate/jsvi

H_∞ control of active vehicle suspensions with actuator time delay

Haiping Du*, Nong Zhang

Mechatronics and Intelligent Systems, Faculty of Engineering, University of Technology, Sydney, P.O. Box 123, Broadway, NSW 2007, Australia

Received 6 January 2006; received in revised form 22 September 2006; accepted 26 September 2006
Available online 13 November 2006

Abstract

The paper deals with the H_∞ control problem for active vehicle suspension systems with actuator time delay. The time delay for the actuator is assumed as uncertain time-invariant but has a known constant bound. By suitably formulating the sprung mass acceleration, suspension deflection and tyre deflection as the optimization object and considering the actuator time delay, a delay-dependent memoryless state feedback H_∞ controller is designed in terms of the feasibility of certain delay-dependent matrix inequalities. A quarter-car model with active suspension system is considered in this paper and a numerical example is employed to illustrate the effectiveness of the proposed approach. It is confirmed by the simulations that the designed controller not only can achieve the optimal performance for active suspensions but also preserves the closed-loop stability in spite of the existence of the actuator time delay within allowable bound.

1. Introduction

Vehicle suspensions play an important role in modern vehicles to improve the compromise among the conflicting vehicle suspension performances, such as ride comfort, road holding, and suspension deflection. A considerable amount of research has been carried out for the last few decades to improve vehicle suspensions [1]. Among the proposed solutions, active suspension is a possible way to improve suspension performance and has attracted much attention [2]. The goal in active suspension control research is to improve the ride performance, generally quantified by sprung mass acceleration, while maintaining an acceptable level of suspension stroke and tyre deflection as packaging and handling measures. Various approaches have been proposed to improve the performance of active suspension designs, such as linear optimal control [3], fuzzy logic and neural network control [4], adaptive control [5], H_∞ control [6], nonlinear control [7], gain-scheduling control [8] and preview control [9], etc. Also, many approaches are presented to deal with the multiobjective requirement of vehicle suspensions (see, e.g., Refs. [10,11] and the references therein). In particular, H_∞ control of active suspensions are intensively discussed in the context of robustness and disturbance attenuation [12–14]. It confirms that H_∞ control of active suspension systems using the

*Corresponding author.
E-mail addresses: hdu@eng.uts.edu.au (H. Du), nong.zhang@uts.edu.au (N. Zhang).

0022-460X/$ - see front matter
doi:10.1016/j.jsv.2006.09.022

optimisation of either a weighted single objective functional with hard constrains or multiobjective functional is an effective way to deal with the conflicting vehicle suspension performance problem.

In active control of vehicle suspension systems, the time delay of the system is another important issue that needs careful treatment to avoid poor performance or even possible instability of the closed-loop system. Time delay or transportation lag is a characteristic that commonly encountered in various engineering systems [15], such as pneumatic and hydraulic systems, chemical processes, long transmission lines, for instance. For active vehicle suspension systems, unavoidable time delays may appear in the controlled channel, particularly in the digital controller as it carries out the calculations associated with complex sophisticated control law, and in sensors and actuators hardware such as hydraulic actuators where the delays are taken by the actuators to build up the required control force. Though the delay time may be short, it can nevertheless limit the control performance or even cause the instability of the system when the delay appears in the feedback loop. For those dynamic systems subjected to a retarded feedback force, the performance and stability of the systems have been studied through characteristic equation analysis [16–18], while the controller synthesis problems and their related issues have not been fully addressed in these studies. The stability and performance of the system due to a retarded control force have been studied only after the controller was designed. In other words, the time delay is not considered when designing the controller in the reported works. Therefore, improvement of performance is expected if the existing time delay of the system can be included in the control design. While such a treatment can be complicated when implementing classical continuous optimal control, the stability analysis and controller synthesis theory for time delay systems have been treated to a great extent recently. For example, the robust H_∞ control problem for uncertain linear systems with multiple state delays and input delays were studied in Refs. [19–22] where delay-dependent or delay-independent control results were obtained; robust stabilization problem for uncertain time-delay systems was studied by Li and de Souza [23] and Moon et al. [24]; the uncertain systems with time-delay and input nonlinearity were dealt in Refs. [25,26]; guaranteed cost control of uncertain time-delay systems can be found in Ref. [27]; and basic theories about robust control of time-delay systems were summarized in Ref. [28], and references therein. This also brings a new issue to controller synthesis for active vehicle suspensions such that the designed controller should be robust with respect to the time delay effect. Recently, attempts to investigate the presence of the time delay in actuator dynamics for active suspensions have been made [29,30]. Although only a few publications have addressed the effect of time delay in active suspension control, this represents a more realistic view in actuator modelling and may have a major effect on the control performance of the suspension system.

Although the H_∞ control law has been employed to improve the performance and robustness of active suspensions effectively, previous works are invariably designed under an implicit assumption that the control inputs can be instantly realized without any delay which, however, is impossible due to many physical limitations in controller implementation. This paper is concerned with the H_∞ controller design problems for a class of vehicle suspension system with time delay in control input. A quarter-car model is used to study the performance of a vehicle suspension system in terms of the bouncing motion, the tyre deflection, and other performance features [30]. Three main performance requirements for advanced vehicle suspensions (ride comfort, road holding, and suspension deflection) are considered by constructing an appropriate state feedback H_∞ controller to provide a trade-off between these requirements. By referring to Ref. [31], where a method that was regarded as the most efficient one in the vast literature to derive the upper bound for the inner product of two vectors was presented, and exploiting the technique in Ref. [20] to deal with input delay, this paper is focused on developing methods to design a state feedback control law based on matrix inequalities such that the closed-loop system is asymptotically stable with a prescribed level of disturbance attenuation subject to input delay within a known bound. Using an iteration algorithm presented in Ref. [31], the feasible solutions can be obtained by linear matrix inequalities (LMIs) using standard numerical algorithms. The designed controller is applied to improve the performance of a quarter-car model. Simulation results on both bump road response and random road response show that in spite of the time delay, the designed state feedback controller can achieve good vehicle suspension performance.

The rest of this paper is organized as follows. Section 2 presents the description of a class of suspension systems being studied. The formulation of a H_∞ control problem for a quarter-car model is given in Section 3. The main results of this paper are given in Section 4 in which a delay-dependent state feedback H_∞ control law can be obtained based on the solvability of matrix inequalities. Section 5 presents the design results and discussions. Finally, we conclude our findings in Section 6.

2. Suspension modelling with actuator time delay

The quarter car model shown in Fig. 1 is considered here for designing active suspension control laws. This model has been used extensively in the literature and captures many important characteristics of more detailed models. To derive the equation of motion of the model, the effect of the actuator dynamics is neglected and the actuator is modelled as an ideal force generator. However, the actuator's delay can be considered as a part of the time delay assumed in the control loop.

The governing equations of motion for the sprung and unsprung masses are:

$$\begin{aligned} &m_s\ddot{z}_s(t) + c_s[\dot{z}_s(t) - \dot{z}_u(t)] + k_s[z_s(t) - z_u(t)] = u(t-\tau), \\ &m_u\ddot{z}_u(t) + c_s[\dot{z}_u(t) - \dot{z}_s(t)] + k_s[z_u(t) - z_s(t)] + k_t[z_u(t) - z_r(t)] + c_t[\dot{z}_u(t) - \dot{z}_r(t)] = -u(t-\tau), \end{aligned} \tag{1}$$

where $z_s(t)$, $z_u(t)$ are the displacements of the sprung and unsprung masses, respectively; m_s is the sprung mass, which represents the car chassis; m_u is the unsprung mass, which represents the wheel assembly; c_s, k_s are damping and stiffness of the passive suspension system, respectively; k_t and c_t stand for compressibility and damping of the pneumatic tyre, respectively; $z_r(t)$ is the road displacement input; $u(t)$ represents the active control force of the suspension system. This control force is normally generated by means of a hydraulic actuator placed between the two masses; τ is the control input time delay. We assume that $z_s(t)$, $z_u(t)$ are measured from their static equilibrium positions and that the tyre remains in contact with the road at all times.

Defining the state variables as follows:

$$\begin{aligned} x_1(t) &= z_s(t) - z_u(t), \\ x_2(t) &= z_u(t) - z_r(t), \\ x_3(t) &= \dot{z}_s(t), \\ x_4(t) &= \dot{z}_u(t), \end{aligned} \tag{2}$$

where $x_1(t)$ denotes the suspension deflection, $x_2(t)$ is the tyre deflection, $x_3(t)$ is the sprung mass speed, and $x_4(t)$ denotes the unsprung mass speed. By defining $x(t) = [x_1(t)\ \ x_2(t)\ \ x_3(t)\ \ x_4(t)]^{\mathrm{T}}$, the equation (1) can be

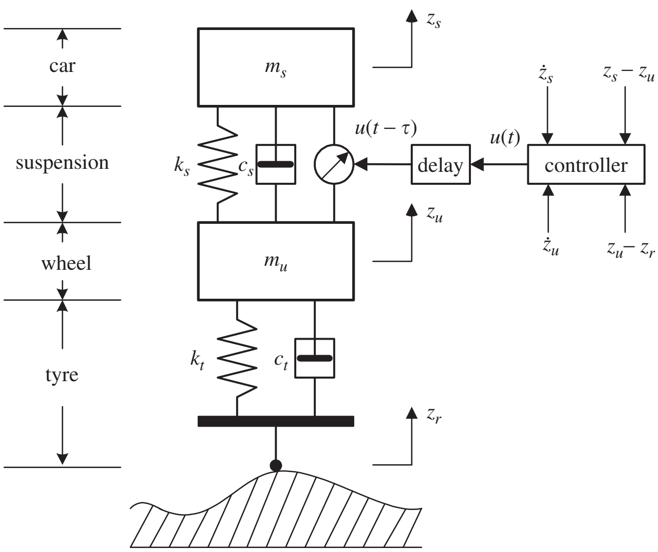

Fig. 1. Quarter-car model with active suspension.

written as

$$\dot{x}(t) = \begin{bmatrix} 0 & 0 & 1 & -1 \\ 0 & 0 & 0 & 1 \\ -k_s/m_s & 0 & -c_s/m_s & c_s/m_s \\ k_s/m_u & -k_t/m_u & c_s/m_u & -(c_s+c_t)/m_u \end{bmatrix} x(t) + \begin{bmatrix} 0 \\ -1 \\ 0 \\ c_t/m_u \end{bmatrix} \dot{z}_r(t) + \begin{bmatrix} 0 \\ 0 \\ 1/m_s \\ -1/m_u \end{bmatrix} u(t-\tau),$$

which can be further expressed by

$$\dot{x}(t) = Ax(t) + B_1 w(t) + B_2 u(t-\tau), \tag{3}$$

where

$$A = \begin{bmatrix} 0 & 0 & 1 & -1 \\ 0 & 0 & 0 & 1 \\ -k_s/m_s & 0 & -c_s/m_s & c_s/m_s \\ k_s/m_u & -k_t/m_s & c_s/m_s & -(c_s+c_t)/m_s \end{bmatrix}, \quad B_1 = [0 \;\; -1 \;\; 0 \;\; c_t/m_u]^{\mathrm{T}},$$

$$B_2 = [0 \;\; 0 \;\; 1/m_s \;\; -1/m_u]^{\mathrm{T}}, \quad w(t) = \dot{z}_r(t).$$

3. Formulation of H_∞ control problem for suspension system

Ride comfort, road holding ability and suspension deflection are three main performance criteria in any vehicle suspension design. It is widely accepted that ride comfort is closely related to the vertical acceleration experienced by the car body. Consequently, in order to improve ride comfort it is important to keep the transfer characteristic from road disturbance, $z_r(t)$, to car body (sprung mass) acceleration, $\ddot{z}_s(t)$, small over the frequency range of 0–65 rad/s [8]. Due to the disturbances caused by road bumpiness, a firm uninterrupted contact of wheels with road (good road holding) is important for vehicle handling and is essentially related to driving safety. To ensure good road holding, it is required that the transfer function from road disturbance, $z_r(t)$, to tyre deflection, $z_u(t) - z_r(t)$, to be small. The structural features of the vehicle also constrains the amount of suspension deflection, $z_s(t) - z_u(t)$, with a hard limit. Hitting the deflection limit not only results in the rapid deterioration in the ride comfort, but at the same time increases the wear of the vehicle. Hence, it is also important to keep the transfer function from road disturbance, $z_r(t)$, to suspension deflection, $z_s(t) - z_u(t)$, small enough to prevent excessive suspension bottoming.

In accordance with the aforementioned requirements, we formulate an H_∞ control problem to deal with the three different objectives for vehicle suspensions. It is standard in the H_∞ framework to use weighting functions to shape and compromise different performance objectives. In order to satisfy the performance requirement, the controlled output $z(t)$ is composed of $\ddot{z}_s(t)$, $z_s(t) - z_u(t)$, and $z_u(t) - z_r(t)$, for the quarter-car model. We consider the case that all the state variables defined in Eq. (2) can be measured, which means that we can design a state feedback H_∞ controller. Therefore, the vehicle suspension control system can be described by equations of the form

$$\begin{aligned} \dot{x}(t) &= Ax(t) + B_1 w(t) + B_2 u(t-\tau), \\ z(t) &= C_1 x(t) + D_{12} u(t-\tau), \\ y(t) &= C_2 x(t), \end{aligned} \tag{4}$$

where $x(t)$, $w(t)$, A, B_1, B_2 are defined as in Eq. (3); $u(t)$ is the control input; $z(t)$ is the controlled output; $y(t)$ is the measured output; with

$$C_1 = \begin{bmatrix} -k_s/m_s & 0 & -c_s/m_s & c_s/m_s \\ \alpha & 0 & 0 & 0 \\ 0 & \beta & 0 & 0 \end{bmatrix}, \quad C_2 = I, \quad D_{12} = [1/m_s \;\; 0 \;\; 0]^{\mathrm{T}}, \tag{5}$$

where $\alpha > 0$ and $\beta > 0$ are scalar weightings for the suspension deflection and tyre deflection, respectively. These weightings are used to control the trade-off between the control objectives.

For the design of an H_∞ controller, we are interested in designing a memoryless state feedback controller

$$u(t) = Ky(t) = Kx(t), \tag{6}$$

where K is the state feedback gain matrix to be designed, such that

(1) the closed-loop system is asymptotically stable;
(2) the closed-loop system guarantees, under zero initial condition, $\|z(t)\|_2 < \gamma \|w(t)\|_2$ for all nonzero $w(t) \in L_2[0, \infty)$ and some prescribed constant $\gamma > 0$.

4. Delay-dependent H_∞ controller design

The following theorem presents the sufficient conditions for the existence of a delay-dependent H_∞ state feedback controller.

Theorem 1. *Consider the suspension system* (4) *and the Appendix A. Given scalar* $\bar{\tau} > 0$, *the closed-loop system of* (4) *is asymptotically stable with* H_∞ *performance index* γ *for any constant time-delay* τ *satisfying* $0 \leqslant \tau \leqslant \bar{\tau}$, *if there exist matrices* $L > 0$, $R > 0$, $W > 0$, M, *and* N, *satisfying matrix inequalities* (7) *and* (8). *Moreover, a desired* H_∞ *state feedback control law is given by* $u(t) = VL^{-1}x(t)$:

$$\begin{bmatrix} LA^{\mathrm{T}} + AL + \bar{\tau}M + N + N^{\mathrm{T}} + W & B_2V - N & B_1 & \bar{\tau}LA^{\mathrm{T}} & LC_1^{\mathrm{T}} \\ * & -W & 0 & \bar{\tau}V^{\mathrm{T}}B_2^{\mathrm{T}} & V^{\mathrm{T}}D_{12}^{\mathrm{T}} \\ * & * & -\gamma^2 I & \bar{\tau}B_1^{\mathrm{T}} & 0 \\ * & * & * & -\bar{\tau}R & 0 \\ * & * & * & * & -I \end{bmatrix} < 0, \tag{7}$$

$$\begin{bmatrix} M & N \\ N^{\mathrm{T}} & LR^{-1}L \end{bmatrix} > 0. \tag{8}$$

Proof. System (4) with the state feedback control law $u(t) = Kx(t)$ becomes

$$\dot{x}(t) = Ax(t) + B_1w(t) + B_2Kx(t-\tau), \tag{9}$$

$$z(t) = C_1x(t) + D_{12}Kx(t-\tau), \tag{10}$$

$$x(t) = \phi(t), \quad \forall t \in [-\tau, 0], \tag{11}$$

where $\phi(t)$ is the initial condition. By the Leibniz–Newton formula and from Eq. (11), it is possible to write

$$x(t-\tau) = x(t) - \int_{t-\tau}^{t} \dot{x}(\theta)\,\mathrm{d}\theta. \tag{12}$$

Substituting $x(t-\tau)$ into Eq. (9) gives

$$\dot{x}(t) = (A + B_2K)x(t) - B_2K\int_{t-\tau}^{t} \dot{x}(\theta)\,\mathrm{d}\theta + B_1w(t). \tag{13}$$

Choose a Lyapunov functional $V(x(t))$ as

$$V(x(t)) \triangleq V_1 + V_2 + V_3, \tag{14}$$

where

$$V_1 \triangleq x^{\mathrm{T}}(t)Px(t), \tag{15}$$

$$V_2 \triangleq \int_{-\tau}^{0}\int_{t+\beta}^{t} \dot{x}^{\mathrm{T}}(\alpha)Z\dot{x}(\alpha)\,\mathrm{d}\alpha\,\mathrm{d}\beta, \tag{16}$$

$$V_3 \triangleq \int_{t-\tau}^{0}\int_{t+\beta}^{t} x^{\mathrm{T}}(\alpha)Qx(\alpha)\,\mathrm{d}\alpha\,\mathrm{d}\beta \tag{17}$$

and $P = P^{\mathrm{T}} > 0$, $Z = Z^{\mathrm{T}} > 0$, $Q = Q^{\mathrm{T}} > 0$ are matrices to be chosen. We take the derivative of V_1 along the state trajectory of system (13) as

$$\begin{aligned}\dot{V}_1 &= x^{\mathrm{T}}(t)[(A+B_2K)^{\mathrm{T}}P + P(A+B_2K)]x(t) - 2x^{\mathrm{T}}(t)PB_2K\int_{t-\tau}^{t}\dot{x}(\theta)\,\mathrm{d}\theta \\ &\quad + w^{\mathrm{T}}(t)B_1^{\mathrm{T}}Px(t) + x^{\mathrm{T}}(t)PB_1w(t).\end{aligned}$$

Define $a(\cdot) \triangleq x(t)$, $b(\cdot) \triangleq \dot{x}(\theta)$, $\mathcal{N} \triangleq PB_2K$ in Lemma B.1 in Appendix B and apply Lemma 1, we obtain

$$\begin{aligned}-2x^{\mathrm{T}}(t)\mathcal{N}\int_{t-\tau}^{t}\dot{x}(\alpha)\,\mathrm{d}\alpha &\leqslant \int_{t-\tau}^{t}\begin{bmatrix} x(t) \\ \dot{x}(\alpha)\end{bmatrix}^{\mathrm{T}}\begin{bmatrix} X & Y-\mathcal{N} \\ Y^{\mathrm{T}}-\mathcal{N}^{\mathrm{T}} & Z\end{bmatrix}\begin{bmatrix} x(t) \\ \dot{x}(\alpha)\end{bmatrix}\mathrm{d}\alpha \\ &= \int_{t-\tau}^{t}[x^{\mathrm{T}}(t)Xx(t) + 2x^{\mathrm{T}}(t)(Y-\mathcal{N})\dot{x}(\alpha) + \dot{x}^{\mathrm{T}}(\alpha)Z\dot{x}(\alpha)]\,\mathrm{d}\alpha \\ &= \tau x^{\mathrm{T}}(t)Xx(t) + 2x^{\mathrm{T}}(t)(Y-\mathcal{N})\int_{t-\tau}^{t}\dot{x}(\alpha)\,\mathrm{d}\alpha + \int_{t-\tau}^{t}\dot{x}(\alpha)Z\dot{x}(\alpha)\,\mathrm{d}\alpha \\ &\leqslant \bar{\tau}x^{\mathrm{T}}(t)Xx(t) + 2x^{\mathrm{T}}(t)(Y-PB_2K)[x(t)-x(t-\tau)] + \int_{t-\tau}^{t}\dot{x}(\alpha)Z\dot{x}(\alpha)\,\mathrm{d}\alpha\end{aligned} \tag{18}$$

and

$$\begin{bmatrix} X & Y \\ Y^{\mathrm{T}} & Z\end{bmatrix} \geqslant 0. \tag{19}$$

Therefore, with conditions (18)–(19), we obtain

$$\begin{aligned}\dot{V}_1 &\leqslant x^{\mathrm{T}}(t)(A^{\mathrm{T}}P + PA + \bar{\tau}X + Y + Y^{\mathrm{T}})x(t) + 2x^{\mathrm{T}}(t)(PB_2K - Y)x(t-\tau) \\ &\quad + w^{\mathrm{T}}(t)B_1^{\mathrm{T}}Px(t) + x^{\mathrm{T}}(t)PB_1w(t) + \int_{t-\tau}^{t}\dot{x}(\alpha)Z\dot{x}(\alpha)\,\mathrm{d}\alpha.\end{aligned} \tag{20}$$

The derivative of V_2 is

$$\begin{aligned}\dot{V}_2 &= \tau\dot{x}^{\mathrm{T}}(t)Z\dot{x}(t) - \int_{t-\tau}^{t}\dot{x}(\alpha)Z\dot{x}(\alpha)\,\mathrm{d}\alpha \\ &\leqslant \bar{\tau}[Ax(t) + B_1w(t) + B_2Kx(t-\tau)]^{\mathrm{T}}Z[Ax(t) + B_1w(t) + B_2Kx(t-\tau)] \\ &\quad - \int_{t-\tau}^{t}\dot{x}(\alpha)Z\dot{x}(\alpha)\,\mathrm{d}\alpha\end{aligned} \tag{21}$$

and the derivative of V_3 is

$$\dot{V}_3 = x^{\mathrm{T}}(t)Qx(t) - x^{\mathrm{T}}(t-\tau)Qx(t-\tau). \tag{22}$$

Combine Eqs. (20)–(22), we have

$$\begin{aligned}\dot{V} &= \dot{V}_1 + \dot{V}_2 + \dot{V}_3 \\ &\leqslant x^{\mathrm{T}}(t)(A^{\mathrm{T}}P + PA + \bar{\tau}X + Y + Y^{\mathrm{T}})x(t) + 2x^{\mathrm{T}}(t)(PB_2K - Y)x(t-\tau) \\ &\quad + \bar{\tau}[Ax(t) + B_1w(t) + B_2Kx(t-\tau)]^{\mathrm{T}}Z[Ax(t) + B_1w(t) + B_2Kx(t-\tau)] \\ &\quad + x^{\mathrm{T}}(t)Qx(t) - x^{\mathrm{T}}(t-\tau)Qx(t-\tau) + w^{\mathrm{T}}(t)B_1^{\mathrm{T}}Px(t) + x^{\mathrm{T}}(t)PB_1w(t).\end{aligned} \tag{23}$$

Assume zero initial condition, i.e. $\phi(t) = 0, \quad \forall t \in [-\tau, 0]$, we have $V(q(t))|_{t=0} = 0$. Consider the following index:

$$J_{zw} \triangleq \int_0^\infty [z^{\mathrm{T}}(t)z(t) - \gamma^2 w^{\mathrm{T}}(t)w(t)]\,\mathrm{d}t \tag{24}$$

then, for any nonzero $w(t) \in L_2[0, \infty)$ there holds,

$$\begin{aligned} J_{zw} &\leqslant \int_0^\infty [z^{\mathrm{T}}(t)z(t) - \gamma^2 w^{\mathrm{T}}(t)w(t)]\,\mathrm{d}t + V(x(t))|_{t=\infty} - V(x(t))|_{t=0} \\ &= \int_0^\infty [z^{\mathrm{T}}(t)z(t) - \gamma^2 w^{\mathrm{T}}(t)w(t) + \dot{V}(x(t))]\,\mathrm{d}t = \int_0^\infty \eta^{\mathrm{T}}(t)\Pi\eta(t)\,\mathrm{d}t, \end{aligned} \tag{25}$$

where $\eta(t) = [x(t) \;\; x(t-\tau) \;\; w(t)]^{\mathrm{T}}$ and

$$\Pi = \begin{bmatrix} \Phi & PB_2K - Y + \bar{\tau}A^{\mathrm{T}}ZB_2K + C_1^{\mathrm{T}}D_{12}K & \bar{\tau}A^{\mathrm{T}}ZB_1 + PB_1 \\ * & -Q + \bar{\tau}K^{\mathrm{T}}B_2^{\mathrm{T}}ZB_2K + K^{\mathrm{T}}D_{12}^{\mathrm{T}}D_{12}K & \bar{\tau}K^{\mathrm{T}}B_2^{\mathrm{T}}ZB_1 \\ * & * & -\gamma^2 I + \bar{\tau}B_1^{\mathrm{T}}ZB_1 \end{bmatrix}, \tag{26}$$

where

$$\Phi = A^{\mathrm{T}}P + PA + \bar{\tau}X + Y + Y^{\mathrm{T}} + Q + \bar{\tau}A^{\mathrm{T}}ZA + C_1^{\mathrm{T}}C_1.$$

When assuming the zero-disturbance input, i.e. $w(t) \equiv 0$, if Eq. (26) is negative-definite, i.e. $\Pi < 0$, then $\dot{V}(x(t)) < 0$ and the asymptotic stability of system (9) is established. When $w(t) \in L_2[0, \infty)$ and $\Pi < 0$ then implies that $J_{zw} < 0$ and therefore $\|z(t)\|_2^2 < \gamma^2\|w(t)\|_2^2$.

By Schur complement, $\Pi < 0$ is equivalent to

$$\begin{bmatrix} A^{\mathrm{T}}P + PA + \bar{\tau}X + Y + Y^{\mathrm{T}} + Q & PB_2K - Y & PB_1 & \bar{\tau}A^{\mathrm{T}}Z & C_1^{\mathrm{T}} \\ * & -Q & 0 & \bar{\tau}K^{\mathrm{T}}B_2^{\mathrm{T}}Z & K^{\mathrm{T}}D_{12}^{\mathrm{T}} \\ * & * & -\gamma^2 I & \bar{\tau}B_1^{\mathrm{T}}Z & 0 \\ * & * & * & -\bar{\tau}Z & 0 \\ * & * & * & * & -I \end{bmatrix} < 0. \tag{27}$$

Define $L \triangleq P^{-1}$, pre- and post-multiplying Eq. (27) by $\mathrm{diag}(L \;\; L \;\; I \;\; Z^{-1} \;\; I)^{\mathrm{T}}$ and its transpose, respectively, we obtain

$$\begin{bmatrix} LA^{\mathrm{T}} + AL + \bar{\tau}LXL + LYL + LY^{\mathrm{T}}L + LQL & B_2KL - LYL & B_1 & \bar{\tau}LA^{\mathrm{T}} & LC_1^{\mathrm{T}} \\ * & -LQL & 0 & \bar{\tau}LK^{\mathrm{T}}B_2^{\mathrm{T}} & LK^{\mathrm{T}}D_{12}^{\mathrm{T}} \\ * & * & -\gamma^2 I & \bar{\tau}B_1^{\mathrm{T}} & 0 \\ * & * & * & -\bar{\tau}Z^{-1} & 0 \\ * & * & * & * & -I \end{bmatrix} < 0. \tag{28}$$

After substituting $V \triangleq KL$, $M \triangleq LXL$, $N \triangleq LYL$, $W \triangleq LQL$, $R \triangleq Z^{-1}$ into Eq. (28), we obtain Eq. (7).

Similarly, pre- and post-multiplying Eq. (19) by $\mathrm{diag}(L \;\; L)^{\mathrm{T}}$ and its transpose, respectively, we obtain

$$\begin{bmatrix} LXL & LYL \\ LY^{\mathrm{T}}L & LZL \end{bmatrix} \geqslant 0 \tag{29}$$

and substitute $M \triangleq LXL$, $N \triangleq LYL$, $R \triangleq Z^{-1}$ into Eq. (29), we obtain Eq. (8).

Conditions (7) and (8) guarantee $\Pi < 0$, which further implies that $J_{zw} < 0$ in Eq. (24), and therefore, the following holds $\int_0^\infty z^{\mathrm{T}}(t)z(t)\,\mathrm{d}t < \int_0^\infty \gamma^2 w^{\mathrm{T}}(t)w(t)\,\mathrm{d}t$ and yields $\|z(t)\|_2^2 < \gamma^2\|w(t)\|_2^2$ for all $w(t) \in L_2[0, \infty)$. This completes the proof. $\square$

5. Application to vehicle active suspension control

In this section, we will apply the proposed approach to design a delay-dependent state feedback H_∞ suspension controller based on the quarter-car model described in Section 2. The quarter-car model parameters have the following values [30]:

$$m_s = 972.2\,\text{kg}, \quad m_u = 113.6\,\text{kg},$$

$$k_s = 42719.6\,\text{N/m}, \quad c_s = 1095\,\text{Ns/m},$$

$$k_t = 101115\,\text{N/m}, \quad c_t = 14.6\,\text{Ns/m}.$$

For subsequent comparison, a delay-dependent state feedback H_∞ controller for system (4) is designed at first. This controller is implemented based on the assumption that all the state variables defined in Eq. (2) can be measured. This controller can be designed by setting $C_2 = I$ and solving the matrices inequalities (7) and (8) for matrices $L>0$, $R>0$, $W>0$, M, and N with a given scalar $\gamma>0$ and $\bar{\tau}$. By setting $\gamma = 11$, $\alpha = 21$, and $\beta = 42$, we obtain the following controller gain matrix based on $K = VL^{-1}$:

$$K = 10^4 \times [-0.3292 \quad -0.6361 \quad -1.0125 \quad -0.0020].$$

For description in brevity, we denote this designed controller as Controller I thereafter. Actually, using the iteration algorithms presented in Ref. [31], Controller I is feasible for the maximum time-delay as $\bar{\tau} = 26\,\text{ms}$. This means that Controller I can stabilize the system (4) with the H_∞ performance index $\gamma = 11$ for any time-delay satisfying $0 \leqslant \tau \leqslant 26\,\text{ms}$.

Then, we design another H_∞ state feedback controller which does not consider the time delay problem during the controller design process based on bounded real lemma (BRL). After setting $\gamma = 11$, $\alpha = 21$, and $\beta = 42$, we obtain such a controller gain as:

$$K = 10^4 \times [-8.9220 \quad -0.1447 \quad -3.6650 \quad 0.1491]$$

and we denote this controller as Controller II for brevity.

Typically, evaluation of the vehicle suspension performance is based on the examination of three response quantities within a prespecified frequency range, that is, the sprung mass acceleration $\dot{x}_3(t)$, the suspension deflection $x_1(t)$ between the wheel and the car body, and the tyre deflection $x_2(t)$. In order to evaluate the suspension characteristics with respect to ride comfort, vehicle handling, and working space of the suspension, the variability of the road profiles are taken into account. In the context of vehicle suspension performance, road disturbances can be generally classified as shock and vibration [1]. Shocks are discrete events of relatively short duration and high intensity, cause by, for example, a pronounced bump or pothole on an otherwise smooth road. Vibrations, on the other hand, are consistent and typically specified as random process with a given ground displacement power spectral density (PSD). In the following, two kinds of road profiles are used to validate the performance of the presented control approach and the effect of the time delay on the performance.

5.1. Bump response

Consider the case of an isolated bump in an otherwise smooth road surface, the corresponding ground displacement is given by

$$z_r(t) = \begin{cases} \dfrac{a}{2}\left(1 - \cos\left(\dfrac{2\pi v_0}{l}t\right)\right), & 0 \leqslant t \leqslant \dfrac{l}{v_0}, \\ 0, & t > \dfrac{l}{v_0}, \end{cases} \tag{30}$$

where a and l are the height and the length of the bump. We choose $a = 0.1\,\text{m}$, $l = 2\,\text{m}$ and the vehicle forward velocity as $v_0 = 45$ (km/h).

When there is no time delay on input, i.e. $\tau = 0$, the bump responses of the open-loop system ($u(t) = 0$) and the closed-loop systems which are composed by Controller I and Controller II, respectively, are compared in Figs. 2–4, where Fig. 2 shows the bump response of the sprung mass acceleration, Fig. 3 shows the bump response of the suspension deflection, and Fig. 4 shows the bump response of the tyre deflection. It can be seen from Figs. 2–4 that better responses are obtained for all closed-loop cases when $\tau = 0$. It is confirmed by the simulation results that good bump response quantities for sprung mass acceleration, suspension deflection, and tyre deflection can be guaranteed by using H_∞ control formulation. Also, the closed-loop performance which is realized by Controller I has the similar result to that of Controller II.

Keeping the system used for the above-mentioned simulations unchanged, we introduce the time-delay $\tau = 24\,\mathrm{ms}$ at the control input. Under the same bump road excitation, the responses of the sprung mass acceleration, suspension deflection, and tyre deflection are plotted in Figs. 5–7, respectively, for the above mentioned three systems. In this case, it is observed from Figs. 5–7 that the response of the closed-loop system that is composed by Controller II is becoming unstable, but on the contrary, the Controller I can still stabilize

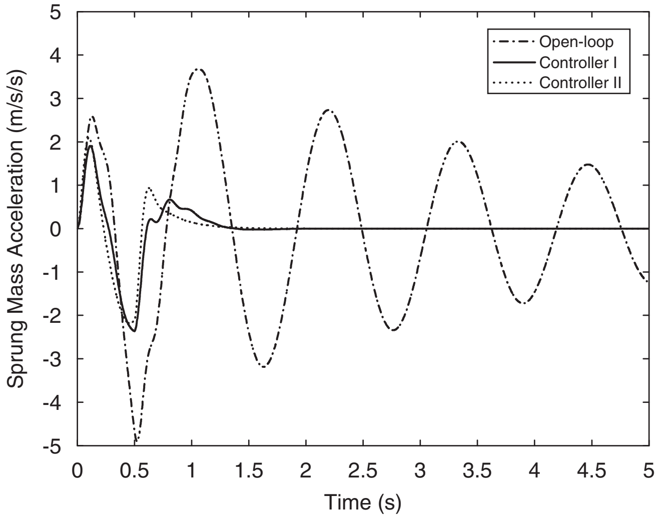

Fig. 2. Bump response of sprung mass acceleration ($\tau = 0\,\mathrm{ms}$).

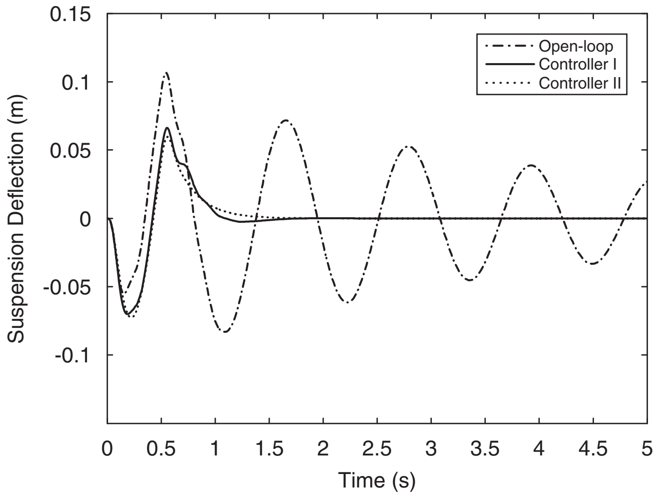

Fig. 3. Bump response of suspension deflection ($\tau = 0\,\mathrm{ms}$).

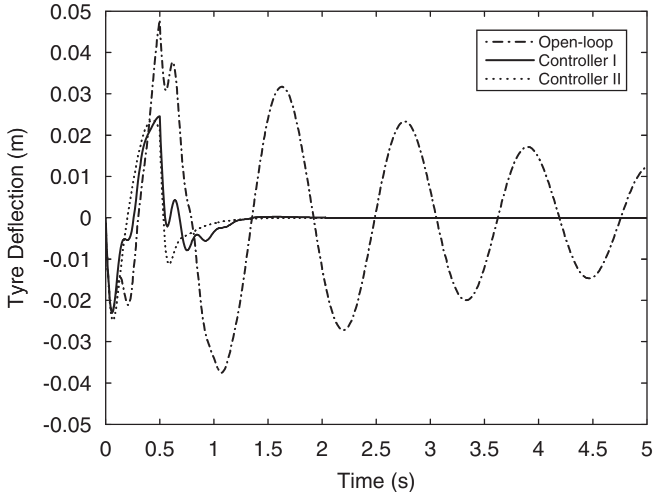

Fig. 4. Bump response of tyre deflection ($\tau = 0\,\text{ms}$).

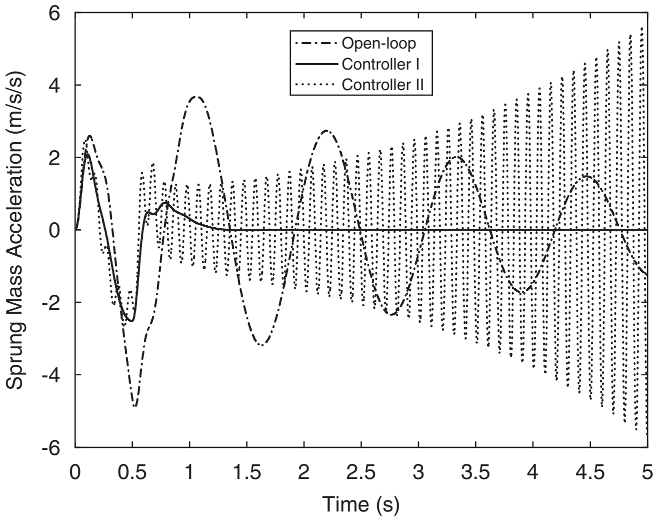

Fig. 5. Bump response of sprung mass acceleration ($\tau = 24\,\text{ms}$).

the closed-loop system with no obvious degradation on performance. It is confirmed that the designed delay-dependent Controller I can tolerate larger time delay in the control input.

5.2. Random response

When the road disturbances are considered as vibrations, they are consistent and typically specified as random process with a ground displacement PSD of

$$S_g(\Omega) = \begin{cases} S_g(\Omega_0)\left(\dfrac{\Omega}{\Omega_0}\right)^{-n_1} & \text{if } \Omega \leqslant \Omega_0, \\ S_g(\Omega_0)\left(\dfrac{\Omega}{\Omega_0}\right)^{-n_2} & \text{if } \Omega \geqslant \Omega_0, \end{cases} \tag{31}$$

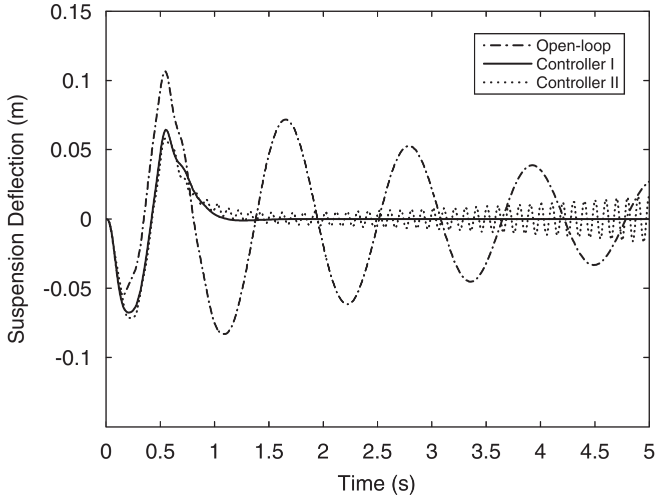

Fig. 6. Bump response of suspension deflection ($\tau = 24\,\text{ms}$).

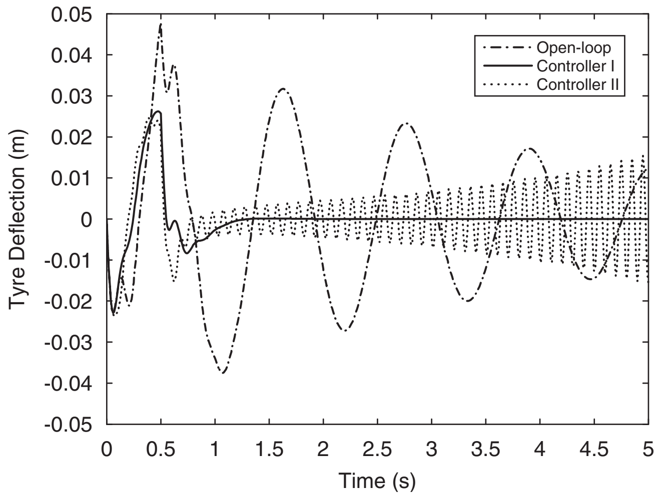

Fig. 7. Bump response of tyre deflection ($\tau = 24\,\text{ms}$).

where $\Omega_0 = 1/2\pi$ is a reference frequency, Ω is a frequency. The value $S_g(\Omega_0)$ provides a measure for the roughness of the road. n_1, n_2 are road roughness constant.

In particular, for vehicle models, samples of the random road profiles are generated using the spectral representation method [32]. If the vehicle is assumed to travel with a constant horizontal speed v_0 over a given road, the road irregularities can be simulated by the following series:

$$z_r(t) = \sum_{n=1}^{N_f} s_n \sin(n\omega_0 t + \varphi_n), \tag{32}$$

where $s_n = \sqrt{2S_g(n\Delta\Omega)\Delta\Omega}$, $\Delta\Omega = 2\pi/l$, l is the length of the road segment, $\omega_0 = (2\pi/l)v_0$, and φ_n is treated as random variables, following a uniform distribution in the interval $[0, 2\pi)$. N_f limits the considered frequency range.

The probabilistic characteristics of the random response are evaluated using Monte Carlo simulation. Taking into account the random nature of the excitation applied, the performance index of root mean square

(RMS) is identified by the following expected values:

$$J_1 = E\left[\frac{1}{T}\int_0^{\mathrm{T}} \{\dot{x}_3(t)\}^2\,\mathrm{d}t\right], \tag{33}$$

$$J_2 = E\left[\frac{1}{T}\int_0^{\mathrm{T}} \{x_1(t)\}^2\,\mathrm{d}t\right], \tag{34}$$

$$J_3 = E\left[\frac{1}{T}\int_0^{\mathrm{T}} \{x_2(t)\}^2\,\mathrm{d}t\right] \tag{35}$$

for sprung mass acceleration, suspension deflection, and tyre deflection, respectively, where $T = l/v_0$ is the temporal measurement period.

To validate the effectiveness of Controller I in dealing with the time delay problem, the effect of different values of time delay in control loop is studied by calculating the RMS ratios $J_i(\tau)/J_i(0)$ and $J_i(\tau)/J_{io}$, $i = 1, 2, 3$, vs. the time-delay τ, where $J_i(\tau)$ denotes the RMS value of the closed-loop system, J_{io} is the RMS value of the open-loop system. We use $n_1 = 2, n_2 = 1.5, v_0 = 20\,\mathrm{m/s}, l = 100, N_f = 200$, in Eqs. (31) and (32) and select the road roughness as $S_g(\Omega_0) = 256 \times 10^{-6}\,\mathrm{m}^3$, which is corresponded to D Grade (Poor) according to ISO 2631 standards, to generate the random road profile. Use $T = 100$ in Eqs. (33)–(35) and randomly run 100 times to calculate the expectation of RMS values for J_1, J_2, and J_3. Fig. 8 shows the plot of the ratio $J_i(\tau)/J_i(0)$, $i = 1, 2, 3$, as a function of the time-delay τ. It is observed from Fig. 8 that there is no significant degradation in the performance of the control system up to the obtained maximal time-delay (26 ms). As the time-delay exceeds about 140 ms, the degradation of the control performance increases. Fig. 9 shows the ratio $J_i(\tau)/J_{io}$, $i = 1, 2, 3$, as a function of the time-delay τ. It can be seen from this figure that the closed-loop performance is better than the open-loop system performance and this good performance can be kept up to about 80 ms with no more degradation in response quantities (the ratios $J_i(\tau)/J_{io}$ are all less than 1 for $i = 1, 2$, and 3 when the time-delay τ is less than about 80 ms). Although the sprung mass acceleration increases a little with the increase of the time-delay τ as shown in Fig. 8, it is still better than the open-loop response when the time-delay τ is less than about 80 ms as shown in Fig. 9. On the other hand, from Figs. 8 and 9, we can observe the conservatism of the presented approach. The designed maximum time-delay is 26 ms, however, the performance and stability of the closed-loop can be kept until the time-delay is about 140 ms.

Now, effect of different values of time delay in the control loop with different road input is studied. To check more random road profiles, we select the road roughness as $S_g(\Omega_0) = 16 \times 10^{-6}\,\mathrm{m}^3$ (B Grade, Good),

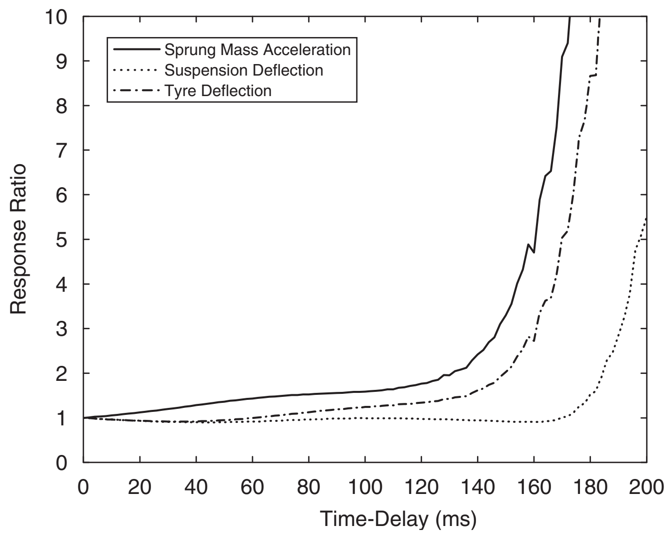

Fig. 8. Random response ratio $J_i(\tau)/J_i(0)$ vs. time-delay τ.

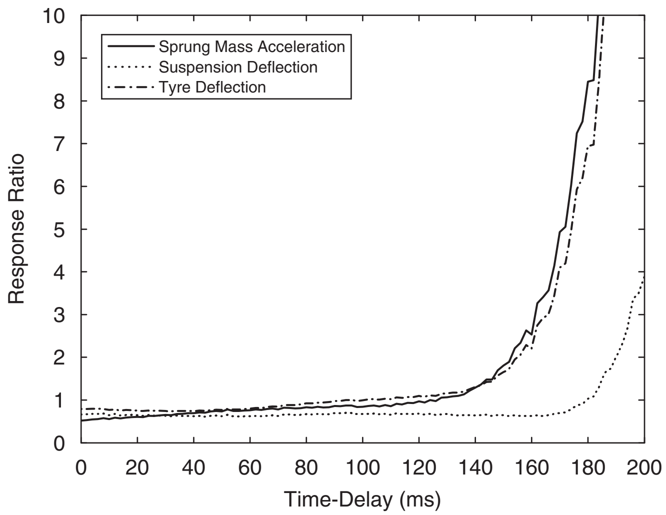

Fig. 9. Random response ratio $J_i(\tau)/J_{io}$ vs. time-delay τ.

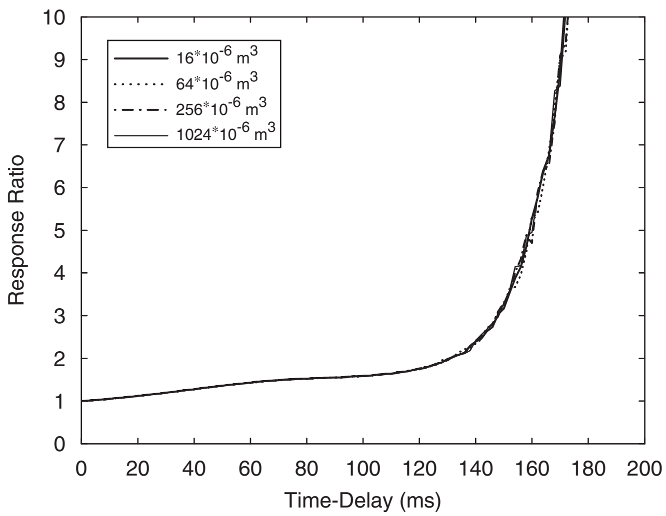

Fig. 10. Random response ratio $J_1(\tau)/J_1(0)$ vs. time-delay τ.

$S_g(\Omega_0) = 64 \times 10^{-6}\,\mathrm{m}^3$ (C Grade, Average), and $S_g(\Omega_0) = 1024 \times 10^{-6}\,\mathrm{m}^3$ (E Grade, Very Poor), respectively, according to ISO 2631 standards, and set $n_1 = 2$, $n_2 = 1.5$, $v_0 = 20\,\mathrm{m/s}$, $l = 100$, $N_f = 200$, $T = 100$ in (31)–(35) and randomly run 100 times to calculate the expectation of RMS values for J_1, J_2, J_3, respectively. The RMS ratios $J_i(\tau)/J_i(0)$, $i = 1, 2, 3$, vs. the time-delay τ, are plotted in Figs. 10–12, respectively, for four kinds of road profiles. It can be observed from Figs. 10–12 that the effect of time delay on the performance is nearly same in spite of the different road roughness.

To show clearly the comparison results between the closed-loop system and the open-loop system, the RMS values for different road roughness and several indicated time-delays, i.e. $\tau = 0$, 20, 40 ms, are compared in Tables 1–3 for sprung mass acceleration, suspension deflection, and tyre deflection, respectively. Since in each case, the road profile is randomly generated independently, the RMS value for every open-loop and closed-loop case can be different. However, the relative performance between the open-loop response and the closed-loop response is nearly same at each given time-delay as shown in Figs. 10–12. Note that the percentage number given in the parentheses indicates the reduced amount of the closed-loop response relative

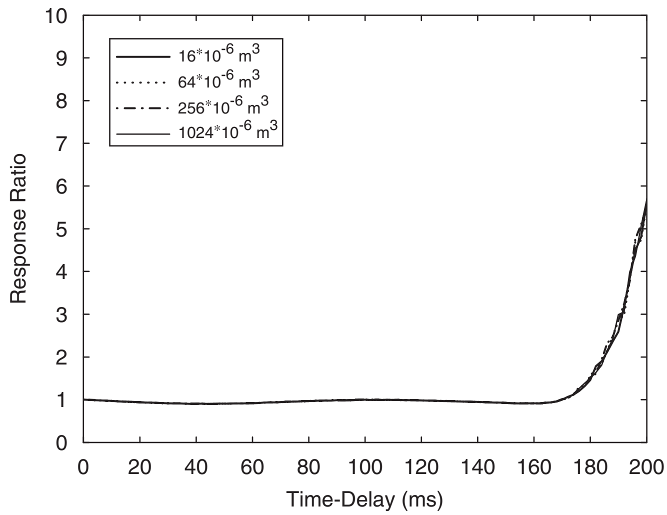

Fig. 11. Random response ratio $J_2(\tau)/J_2(0)$ vs. time-delay τ.

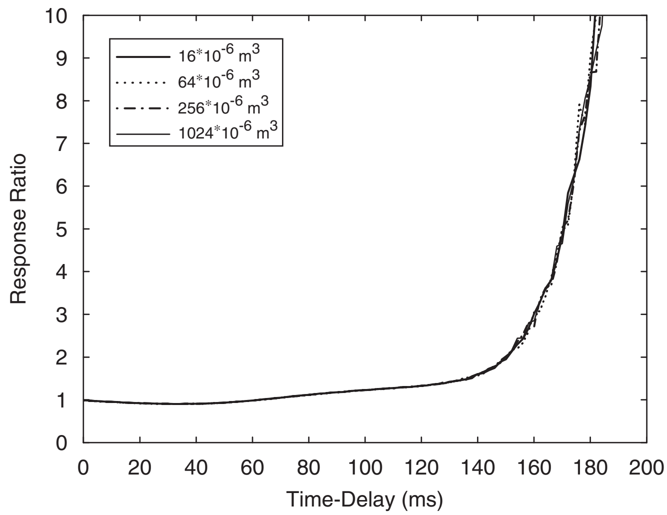

Fig. 12. Random response ratio $J_3(\tau)/J_3(0)$ vs. time-delay τ.

Table 1
Comparison of RMS values of acceleration (m/s^2) for different road roughness and time-delay

Time-delay	$\tau = 0\,\text{ms}$		$\tau = 20\,\text{ms}$		$\tau = 40\,\text{ms}$	
Roughness	Open-loop	Closed-loop	Open-loop	Closed-loop	Open-loop	Closed-loop
$16 \times 10^{-6}\,\text{m}^3$	0.17	0.09 (−46%)	0.17	0.10 (−40%)	0.16	0.12 (−29%)
$64 \times 10^{-6}\,\text{m}^3$	0.33	0.18 (−45%)	0.33	0.20 (−39%)	0.34	0.23 (−31%)
$256 \times 10^{-6}\,\text{m}^3$	0.69	0.36 (−48%)	0.67	0.40 (−39%)	0.67	0.46 (−30%)
$1024 \times 10^{-6}\,\text{m}^3$	1.33	0.72 (−46%)	1.35	0.81 (−40%)	1.33	0.92 (−30%)

Table 2
Comparison of RMS values of suspension deflection (cm) for different road roughness and time-delay

Time-delay	$\tau = 0\,\text{ms}$		$\tau = 20\,\text{ms}$		$\tau = 40\,\text{ms}$	
Roughness	Open-loop	Closed-loop	Open-loop	Closed-loop	Open-loop	Closed-loop
$16 \times 10^{-6}\,\text{m}^3$	0.36	0.24 (−31%)	0.36	0.23 (−36%)	0.34	0.22 (−36%)
$64 \times 10^{-6}\,\text{m}^3$	0.69	0.49 (−29%)	0.71	0.46 (−35%)	0.72	0.44 (−38%)
$256 \times 10^{-6}\,\text{m}^3$	1.48	0.98 (−33%)	1.41	0.92 (−35%)	1.41	0.88 (−37%)
$1024 \times 10^{-6}\,\text{m}^3$	2.81	1.96 (−30%)	2.86	1.83 (−35%)	2.81	1.76 (−37%)

Table 3
Comparison of RMS values of tyre deflection (cm) for different road roughness and time-delay

Time-delay	$\tau = 0\,\text{ms}$		$\tau = 20\,\text{ms}$		$\tau = 40\,\text{ms}$	
Roughness	Open-loop	Closed-loop	Open-loop	Closed-loop	Open-loop	Closed-loop
$16 \times 10^{-6}\,\text{m}^3$	0.22	0.18 (−19%)	0.22	0.17 (−24%)	0.22	0.16 (−24%)
$64 \times 10^{-6}\,\text{m}^3$	0.43	0.36 (−18%)	0.44	0.33 (−24%)	0.44	0.33 (−25%)
$256 \times 10^{-6}\,\text{m}^3$	0.90	0.71 (−20%)	0.88	0.66 (−24%)	0.88	0.65 (−25%)
$1024 \times 10^{-6}\,\text{m}^3$	1.75	1.42 (−18%)	1.76	1.33 (−24%)	1.75	1.31 (−25%)

to the open-loop case in all tables. For instance, the maximum RMS sprung mass acceleration is reduced by about 40% when $\tau = 20\,\text{ms}$ for every road roughness, using the proposed control approach, while at the same time the maximum RMS suspension deflection is about 35% less than that of the open-loop one, implying that a smaller suspension travel space may be used, and the maximum RMS tyre deflection is about 24% less than that of the open-loop one, implying a smaller tyre travel space as well.

Tables 1–3 show that with the increase of time-delay, the proposed control method is still able to effectively control the sprung mass acceleration, suspension deflection, and tyre deflection in lower values.

6. Conclusions

In this paper, we present a delay-dependent H_∞ controller design method for active vehicle suspensions with actuator time delay. The inclusion of time delay in actuator provides a more realistic model for modelling vehicle suspension systems. By referring to the recent result on deriving the upper bound for the inner product of two vectors, the state feedback H_∞ control law is obtained based on the solution of delay-dependent matrix inequalities. The presented controller design approach is no more complex than designing an ordinary state feedback H_∞ controller. However, designing a controller that considers the time delay effect in advance can guarantee the closed-loop performance and stability within allowable time delay bound. A simulation example is used to demonstrate that the designed controller can effectively achieve the optimal vehicle suspension performance even with actuator time delay to a certain extent.

Acknowledgments

The financial support of this work by the Australian Research Council (DP0560077) and the University of Technology, Sydney, is gratefully acknowledged. The authors would like to express thanks to the reviewers for all the valuable comments and suggestions lead to the considerable improvement on the presentation of this paper.

Appendix A

Notation: $\mathbb{R}^n$ denotes the n-dimensional Euclidean space and $\mathbb{R}^{n\times m}$ the set of all $n\times m$ real matrices, $\|\cdot\|$ refers to either the Euclidean vector norm or the induced matrix 2-norm. For a real symmetric matrix W, the notation of $W>0$ ($W<0$) is used to denote its positive- (negative-) definiteness. Also, I is used to denote the identity matrix of appropriate dimensions. To simplify notation, $*$ is used to represent a block matrix which is readily inferred from symmetry.

Appendix B

Lemma B.1. *Assume $a(\cdot)\in\mathbb{R}^{n_a}$, $b(\cdot)\in\mathbb{R}^{n_b}$ and $\mathcal{N}\in\mathbb{R}^{n_a\times n_b}$ are defined on the interval Ω. Then for any matrices $X\in\mathbb{R}^{n_a\times n_b}$, $Y\in\mathbb{R}^{n_a\times n_b}$ and $Z\in\mathbb{R}^{n_a\times n_b}$, the following holds*:

$$-2\int_{\Omega} a^{\mathrm{T}}(\alpha)\mathcal{N}b(\alpha)\,\mathrm{d}\alpha \leqslant \int_{\Omega}\begin{bmatrix} a(\alpha)\\ b(\alpha)\end{bmatrix}^{\mathrm{T}}\begin{bmatrix} X & Y-\mathcal{N}\\ Y^{\mathrm{T}}-\mathcal{N}^{\mathrm{T}} & Z\end{bmatrix}\begin{bmatrix} a(\alpha)\\ b(\alpha)\end{bmatrix}\mathrm{d}\alpha,$$

where

$$\begin{bmatrix} X & Y\\ Y^{\mathrm{T}} & Z\end{bmatrix}>0.$$

References

[1] D. Hrovat, Survey of advanced suspension developments and related optimal control applications, *Automatica* 33 (10) (1997) 1781–1817.

[2] R.A. Williams, Automotive active suspensions, *Proceedings of the Institution of Mechanical Engineers Part D: Journal of Automobile Engineering* 211 (1997) 415–444.

[3] M.M. Elmadany, Z.S. Abduljabbar, Linear quadratic Gaussian control of a quarter-car suspension, *Vehicle System Dynamics* 32 (6) (1999) 479–497.

[4] N. Al-Holou, T. Lahdhiri, D.S. Joo, J. Weaver, F. Al-Abbas, Sliding mode neural network inference fuzzy logic control for active suspension systems, *IEEE Transactions on Fuzzy Systems* 10 (2) (2002) 234–246.

[5] I. Fialhm, G.J. Balas, Road adaptive active suspension design using linear parameter-varying gain-scheduling, *IEEE Transactions on Control Systems Technology* 10 (1) (2002) 43–54.

[6] M. Yamashita, K. Fujimori, K. Hayakawa, H. Kimura, Application of H_∞ control to active suspension systems, *Automatica* 30 (11) (1994) 1717–1720.

[7] N. Karlsson, M. Dahleh, D. Hrovat, Nonlinear H_∞ control of active suspensions, *Proceedings of the American Control Conference*, Arlington, VA, USA, 2001, pp. 3329–3334.

[8] I. Fialho, G.J. Balas, Design of nonlinear controllers for active vehicle suspensions using parameter-varying control synthesis, *Vehicle System Dynamics* 33 (5) (2000) 351–370.

[9] A.G. Thompson, C.E.M. Pearce, Performance index for a preview active suspension applied to a quarter-car model, *Vehicle System Dynamics* 35 (1) (2001) 55–66.

[10] E. Abdellari, D. Mehdi, M. M'Saad, On the design of active suspension system by H_∞ and mixed H_∞/H_2: an LMI approach, *Proceedings of the American Control Conference*, Chicago, IL, USA, 2000, pp. 4041–4045.

[11] J. Wang, D.A. Wilson, Mixed $GL_2/H_2/GH_2$ control with pole placement and its application to vehicle suspension systems, *International Journal of Control* 74 (13) (2001) 1353–1369.

[12] H. Du, J. Lam, K.Y. Sze, Design of non-fragile H_∞ controller for active vehicle suspensions, *Journal of Vibration and Control* 11 (2005) 225–243.

[13] H. Chen, K. Guo, Constrained H_∞ control of active suspensions: an LMI approach, *IEEE Transactions on Control Systems Technology* 13 (3) (2005) 412–421.

[14] H. Chen, Z.Y. Liu, P.Y. Sun, Application of constrained H_∞ control to active suspension system on half-car models, *Journal of Dynamic Systems, Measurement, and Control* 127 (2005) 345–354.

[15] K. Gu, S. Niculescu, Survey on recent results in the stability and control of time-delay systems, *Journal of Dynamic Systems, Measurement, and Control* 125 (2003) 158–165.

[16] T. Hong, P.C. Hughes, Effect of time delay on the stability of flexible structures with rate feedback control, *Journal of Vibration and Control* 7 (2001) 33–49.

[17] H.Y. Hu, E.H. Dowell, L.N. Virgin, Stability estimation of high dimensional vibrating systems under state delay feedback control, *Journal of Sound and Vibration* 214 (3) (1998) 497–511.
[18] Z.H. Wang, H.Y. Hu, Delay-independent stability of retarded dynamic systems of multiple degrees of freedom, *Journal of Sound and Vibration* 226 (1) (1999) 57–81.
[19] Y.Y. Cao, Y.X. Sun, J. Lam, Delay-dependent robust H_∞ control for uncertain systems with time-varying delays, *IEE Proceedings: Control Theory and Applications* 145 (3) (1998) 338–344.
[20] X. Li, M. Guay, B. Huang, D.G. Fisher, Delay-dependent robust H_∞ control of uncertain linear systems with input delay, *Proceedings of the American Control Conference*, San Diego, CA, USA, 1999, pp. 800–804.
[21] H. Li, S.I. Niculescu, L. Dugard, J.M. Dion, Robust H_∞ control of uncertain linear time-delay systems: a linear matrix inequality approach, *Proceedings of the 35th Conference on Decision and Control*, Kobe, Japan, 1996, pp. 1370–1375.
[22] H. Du, J. Lam, K.Y. Sze, H_∞ disturbance attenuation for uncertain mechanical systems with input delay, *Transactions of the Institute of Measurement and Control* 27 (1) (2005) 37–52.
[23] X. Li, C.E. deSouza, Delay-dependent robust stability and stabilization of uncertain linear delay systems: a linear matrix inequality approach, *IEEE Transactions on Automatic Control* 42 (8) (1997) 1144–1148.
[24] Y.S. Moon, P.G. Park, W.H. Kwon, Robust stabilization of uncertain input-delayed systems using reduction method, *Automatica* 37 (2001) 307–312.
[25] S. Xu, J. Lam, Robust H_∞ control for uncertain state-delayed systems with sector nonlinearity, *Proceedings of the Institution of Mechanical Engineers Part I: Journal of Systems and Control Engineering* 215 (2001) 511–520.
[26] H.Y. Su, F. Liu, J. Chu, Robust stabilisation of uncertain time-delay systems containing saturating actuators, *IEE Proceedings: Control Theory and Applications* 148 (4) (2001) 323–328.
[27] S.H. Esfahani, S.O.R. Moheimani, I.R. Petersen, LMI approach to suboptimal guaranteed cost control for uncertain time-delay systems, *IEE Proceedings: Control Theory and Applications* 145 (6) (1998) 491–498.
[28] M.S. Mahmoud, *Robust Control and Filtering for Time-delay Systems*, Marcel Dekker, Inc., New York, 2000.
[29] A. Vahidi, A. Eskandarian, Predictive time-delay control of active suspensions, *Journal of Vibration and Control* 7 (2001) 1195–1211.
[30] N. Jalili, E. Esmailzadeh, Optimum active vehicle suspensions with actuator time delay, *Journal of Dynamic Systems, Measurement, and Control* 123 (2001) 54–61.
[31] Y.S. Moon, P.G. Park, W.H. Kwon, Y.S. Lee, Delay-dependent robust stabilization of uncertain state-delayed system, *International Journal of Control* 74 (14) (2001) 1447–1455.
[32] G. Verros, S. Natsiavas, C. Papadimitriou, Design optimization of quarter-car models with passive and semi-active suspensions under random road excitation, *Journal of Vibration and Control* 11 (2005) 581–606.